Journal of Orthopaedic Research

Adolescent obesity incurs adult skeletal deficits in murine induced obesity model

Journal:	*Journal of Orthopaedic Research*
Manuscript ID	JOR-21-0090.R2
Wiley - Manuscript type:	Research Article (Member)
Date Submitted by the Author:	06-Mar-2022
Complete List of Authors:	Shefelbine, Sandra; Northeastern University, Bioengineering; Northeastern University, Mechanical and Industrial Engineering Ben Tahar, Soha; Northeastern University, Bioengineering Garnier, Julien; Northeastern University, Bioengineering Eller, Kerry; Northeastern University, Bioengineering DiMauro, Nicole; Northeastern University, Bioengineering Piet, Judith; Northeastern University, Bioengineering Mehta, Shihkar; Northeastern University, Bioengineering Bajpayee, Ambika; Northeastern University, Bioengineering
Areas of Expertise:	bone, obesity, mechanics, brittleness
Keywords:	Bone, Pediatric

Adolescent obesity incurs adult skeletal deficits in murine induced obesity model

Soha Ben Tahar[1], Julien Garnier[1], Kerry Eller[1], Nicole DiMauro[1], Judith Piet[1]

Shihkar Mehta[1], Ambika G. Bajpayee[1], Sandra J. Shefelbine[1,2]

[1]Department of Bioengineering, [2]Department of Mechanical and Industrial Engineering

Northeastern University, Boston, MA

Running Title: Bone in adolescent obesity

Author Contributions: KE, ND, JP, and SJS designed the study; SBT, JG, KE, ND, JP, SM carried out analysis and analyzed the data; SBT, JG, KE, ND, AGB wrote and revised the manuscript. All authors have read and approved the final manuscript.

Corresponding Author:

Sandra J. Shefelbine

Department of Bioengineering

Department of Mechanical and Industrial Engineering

Northeastern University

Boston, MA

s.shefelbine@northeastern.edu

617-386-3885

Abstract

Adolescent obesity has risen dramatically in the last few decades. While adult obesity may be osteoprotective, the effects of obesity during adolescence, which is a period of massive bone accrual, are not clear. We used a murine model of induced adolescent obesity to examine the structural, mechanical, and compositional differences between obese and healthy weight bone in in 16 week old female C57Bl6 mice. We also examined the effects of a return to normal weight after skeletal maturity (24 week old). We found obese adolescent bone exhibited decreased trabecular bone volume, increased cortical diameter, increased ultimate stress, and increased brittleness (decreased plastic energy to fracture), similar to an aging phenotype. The trabecular bone deficits remained after return to normal weight after skeletal maturity. However after returning to normal diet, there was no difference in ultimate stress nor plastic energy to fracture between groups as the normal diet group increased ultimate stress and brittleness. Interestingly, compositional changes appeared in the former high fat diet mice after skeletal maturity with a lower mineral to matrix ratio compared to normal diet mice. In addition there was a trend toward increased fluorescent advanced glycation endproducts in the former high fat diet mice compared to normal diet mice but this did not reach significance ($p<0.05$) due to the large variability. The skeletal consequences of adolescent obesity may have lasting implications for the adult skeleton even after return to normal weight. Given the rates of adolescent obesity, skeletal health should be a concern.

Keywords: bone, obesity, mechanics, brittleness

Declaration: Nothing to declare.

Introduction

Childhood and adolescent obesity has risen dramatically in recent years. Since the 1970s, obesity rates have tripled in children and adolescents. Obesity now affects 18.5% of the youth aged 2- to 19-years-old in the USA [1]. These figures are alarming as adolescence has a key role for skeletal development; more than 1/4 of adult bone mass is accrued during this crucial period [2]. Moreover, according to recent studies, obese children are overrepresented in fracture groups and have lower bone mass than expected for their height and weight [3]. Yet it is unclear whether the increased risk of fracture is due to an increased risk of falling, increased load upon the bones when falls occur, or structural insufficiency of the bones. In adults, obesity is osteoprotective, resulting in higher bone density and improved bone microarchitecture [4]. However, the effects of obesity on bone during childhood are unclear; some studies indicate an increase in total bone mass [5-7] (in children and adolescents) but when adjusted for bone size, other studies report a decrease in bone density in obese children [5], [8]. High fat diet-induced obesity studies in rodents have indicated an increase in cortical cross sectional parameters (thickness, area, moment of area) [9 ♂, 10 ♀, 11 ♂], and a decrease trabecular bone parameters (trabecular volume fraction, thickness, number) [10 ♀, 12 ♂, 34 ♂] that was dependent on particular mouse strain [35 ♂] compared to healthy weight mice. Some studies have found a decrease in cortical material properties (modulus, yield and ultimate strength) in obese adolescent bone compared to healthy weight bone [13 ♂], while others have found no change [9 ♂, 10 ♀]. Diet-induced adolescent obesity in rodents increases cortical bone, reduces trabecular bone and may affect bone quality. Changes to skeletal health during growth and development may have lasting detrimental consequences into skeletal maturity. Indeed, recent reviews have called for further studies to understand how childhood obesity affects skeletal maturation and development [14]. With the prevalence of obesity rising globally, there is a need to determine its effects on bone health, both immediate and long-term.

We hypothesize that adolescent diet-induced obesity results in structural, mechanical, and compositional changes to bone and that these changes persist after return to normal diet and healthy weight. Even if

obesity is corrected later in life, reductions of bone health during adolescence may have irreparable consequences.

Methods

Induced Obesity Model

38 adolescent C57BL6/J female mice were obtained from JAX. Mice were randomized and housed in groups of five with a 12-hour light/dark cycle. All animal procedures received approval from Northeastern University's Institutional Animal Care and Use Committee (IACUC). 19 mice were fed Rodent Diet with 60 kCal% Fat (Research Diets D12492) from 4-16 weeks of age, and 19 mice were fed a standard mouse diet (ScottPharma). At 16 weeks of age 9 obese mice and 9 control mice were euthanized by carbon dioxide inhalation followed by cervical dislocation. The remaining 10 mice in both groups were fed a normal diet ad libitum for an additional 8 weeks and euthanized at 24 weeks. Mouse weights were recorded weekly. After euthanization, the gonadal fat pad was removed from each mouse and weighed.

We compared the structural, mechanical, and compositional differences in the normal diet (ND) and high fat diet (HFD) mice at 16 weeks of age to determine the short-term effects of adolescent obesity on bone properties. In the 24 week old mice, we compared properties of ND and former high fat diet (FHDF) mice to determine the long term effects of obesity.

Micro-CT imaging

Femurs were dissected and soft tissue was removed. The bones were kept frozen at -20°C in PBS until scanning. Femurs wrapped in PBS soaked gauze and plastic wrap were scanned (Scanco Medical µCT 35) at an isotropic voxel size of 10 µm using an X-ray source power of 70 kVp, an aluminum filter of 0.5mm, an X-ray intensity of 114 µA and an integration time of 400 ms per slice. Structural properties of trabecular and cortical bone were evaluated (Figure 1).

Trabecular bone

Trabecular bone morphology was evaluated in a total of 180 slices in a region starting 360 µm proximal to the distal growth plate and extending 1800 µm proximally [15]. Image segmentation was done using a low- pass Gaussian filter (σ = 1.5) to remove noise and a fixed gray scale threshold of 1900 to isolate mineralized bone. Images were imported into ImageJ [16] and BoneJ plugin [17] was used to measure the morphometric variables trabecular thickness (Tb.Th), trabecular separation (Tb.Sp) and bone volume fraction (BV/TV). The variable trabecular number (Tb.N) was calculated as 1/(Tb.Th + Tb.Sp) [18].

Cortical bone

Cortical bone morphology was evaluated along the shaft in the middle 50% of bone length. Cortical bone was separated from the trabecular structure by manual contouring. Image segmentation was done by using a low-pass Gaussian filter (σ = 0.8) to remove noise and a fixed gray scale threshold of 2800 to isolate mineralized bone. A connectivity analysis was performed with BoneJ to remove remaining particles. Finally, BoneJ was used to align the femurs along the longitudinal axis before analyzing each slice the morphometric variables cross-sectional area (CSA), second moment of area around medio-lateral axis (I_M) and diameter along the medio-lateral axis (D_M).

Mechanical Testing

Left femurs were tested in three-point bending test (Instron 5960) with a constant span length of 8.0 mm. Prior to testing, the femurs were soaked in PBS solution, at room-temperature. The bone was positioned horizontally with the anterior surface in compression and posterior surface in tension. Displacement occurred at a constant speed of 0.5 mm/s until failure.

The stress and strain were calculated from the load-displacement curves according to the formulas:

$$\sigma = \frac{F \times L \times y}{4 \times I_{ML}}$$

$$\epsilon = \frac{12 \times d \times y}{L^2}$$

where F is the applied load, and d is the deflection at the loading point, L is the span distance between the two pins (8 mm), I_{ML} is the moment of inertia around the medio-lateral axis (the axis perpendicular to the loading axis), and y is the maximum distance between the centroid and outer anterior/posterior surface of the bone (the loading axis). I_{ML} and y were determined by averaging 50 slices (0.5 mm) at midshaft.

From the stress-strain curves, we calculated the yield stress (using 0.2% offset method), ultimate stress, elastic modulus, the energy to fracture (area under the stress-strain curve) and the ductility (area under the stress-strain curve in the plastic domain).

Raman Spectroscopy

After 3 point bending, Raman spectra were acquired for the cortical bone of each right femur using a custom fiber-optic Raman spectral probe, as described [19]. The system consisted of a hollow probe connected to a NIR diode laser (λ_{ex} = 785 nm, 500 mW, 200µm fiber, B&W Tek) and a fiber-coupled spectrograph (7 bundled collection fibers of 105µm, 2 cm^{-1} resolution, QEPRO, Ocean Insights), interfaced with distal optic filters and a plano-convex lens (N-BK7, ∅9mm, 10mm focal length). Spectra were acquired over 30 second integration time and averaged over 4 positions within the femur mid-shaft (one anterior and one posterior point on either side of the break). Spectra were subjected to preprocessing, consisting of background subtraction, baseline autofluorescence removal (5th order polynomial fit function), and smoothing (first order Savitzky-Golay, 5 pixel window filter).
The areas under the Amide III (1190-1260 cm^{-1}), Amide I (1530-1640 cm^{-1}), CO_3 (999-1040 cm^{-1}), and ν PO_4 (920-970 cm^{-1}) peaks were calculated (Supplementary Information Figure S1 presents representative spectra). The mineral to matrix ratio was calculated by dividing the area under the phosphate peak by the area under the Amide I peak. The carbonate substitution was calculated by dividing the area under the CO_3 peak by the area under the phosphate peak.

141 *Fluorescent advanced glycation end-products*

142 Fluorescent advanced glycation end-products (AGEs) were quantified using a fluorometric assay analysis
143 on the femurs in ND mice (young and old), HFD mice and FHFD mice (after 3pt bending testing). This is
144 a colorimetric assay based on the oxidation of the hydroxyproline with Chloramine-T and the reaction of
145 the products with p-dimethylaminobenzaldehyde (DMAB). The hydroxyproline content enables us to
146 quantify the amount of collagen in order to normalise the AGE content [19]. From each group, 9 bones
147 were examined.

148 The bones were defatted by submerging the specimens in 100% isopropyl ether. The samples were next
149 lyophilized using a freeze dryer system (Labconco, MO, US) for 24 hours. Samples were hydrolyzed with
150 6N HCl (50 µL per mg of bone) for 20 hours at 110°C. After being hydrolyzed, the HCl was evaporated
151 using a hot plate (60°C). AGE fluorescence was measured for the hydrolysates at 360/460 nm
152 excitation/emission using a microplate reader (Synergy H1, BioTek, VT, US) and calibrated using a
153 Quinine standard.

154 Then the hydroxyproline content was measured to estimate total collagen content [19–21]. Chloramine T
155 was added to serially diluted hydroxyproline standards and bone specimen hydrolysates. The solution was
156 mixed and incubated at room temperature for 20 min. To remove the residual Chloramine-T, 3.15M
157 perchloric acid and DMAB was added and incubated in a water bath at 60°C for 15 minutes. All samples
158 were cooled at room temperature in darkness for 5 mins, and then absorbance was measured at 560 nm
159 using the same microplate reader. The amount of fluorescence from the AGEs was normalized with the
160 hydroxyproline content.

Statistical Analysis

All data were analyzed for normality (Shapiro-Wilks test) and equal variances (F-test) before ANOVA to assess differences among groups. For parameters with unequal variance (ultimate stress in 24 week old mice, fluorescent AGEs at both ages, and carbonate-phosphate ratio in 16 week old mice) a Welch test was used. Post-hoc Tukey HSD was performed to test for differences between groups. We report the differences between ND and HFD within an age group here. Differences across ages (not the focus of the study and widely reported elsewhere) are reported in Supplemental Information.

Results

Body and fat pad weights

The weights of the ND and HFD groups were significantly different from the age of 5 weeks to the time of euthanization at 16 weeks of age (Figure 2). The weights of the two groups were not statistically different after the mice returned to a normal diet. In the 16 week old mice, the fat pads were significantly heavier in HFD mice, compared to ND (0.89 +/- 0.33 g and 0.32+/- 0.12 g respectively, Figure 3). Gonadal fat pads are used as a marker of obesity, so this indicates the HFD successfully induced obesity in the mice. In the 24 week old mice, the fat pads were not significantly different between the ND mice and the FHFD (0.38 ± 0.19g and 0.58 ± 0.34g, respectively). This reflects the fact that after returning to a normal diet, the mice were no longer obese.

Trabecular Structure

Trabecular Number (Tb.N) and Bone Volume Fraction (BV/TV) were significantly lower for 16-week-old HFD mice compared ND mice (Figure 4). In particular, cancellous bone volume was reduced by 39% in 16-week-old HFD mice when compared to same age ND mice. Trabecular Spacing (Tb.Sp) was significantly higher for 16-week-old HFD mice when compared ND mice. These results suggest that high fat diet-induced obesity is linked to a deterioration of the trabecular structure.

185 Tb.Th, Tb.N and BV/TV were found significantly lower for 24-week-old FHFD mice when compared to
186 ND mice (Figure 4). Trabecular Spacing (Tb.Sp) was significantly higher for 24-week-old FHFD mice
187 compared ND mice. These results highlight the lasting effect of high fat diet on trabecular bone structure
188 (Figure 5). After 8 weeks of diet correction, the mice were no longer obese, but trabecular structure was
189 still impaired.

190 ***Cortical Structure***

191 Cross-Sectional Area (CSA) was found significantly higher for 16-week-old HFD mice in the middle and
192 distal parts of the shaft when compared to same age ND mice (Figure 6A). This result suggests that high
193 fat diet is linked to an increase in cortical bone, likely because of the increase in body weight.

194 Moment of area around the medial-lateral axis, I_{ML}, was significantly higher for 16-week-old HFD mice
195 in the middle and distal parts of the diaphysis compared to ND mice. I_{ML} was also significantly higher for
196 24-week-old FHFD mice at the mid-shaft compared to ND mice (Figure 6B).

197 This result was further investigated by studying bone diameter along the medio-lateral axis (D_{ML}). D_{ML}
198 was found significantly higher for 16-week-old HFD mice when compared to same age ND mice. D_{ML}
199 was also found significantly higher for 24-week-old FHFD mice at the mid-shaft when compared to same
200 age ND mice (Figure 6C). Therefore the differences found in CSA and I_{ML} are explained by a higher shaft
201 diameter in HFD mice.

202 *Mechanical Properties*

203 At 16 weeks, compared to the ND group, the yield stress and elastic modulus were similar in HFD
204 ($p>0.05$), but the ultimate stress was significantly higher for HFD ($p=0.006$) and the energy to fracture
205 was significantly lower for HFD ($p<0.005$). The mechanical properties of FHFD mice were not
206 significantly different from the ND group ($p>0.05$). (Figure 7)

Composition

There was no significant difference in mineral to matrix ratio and carbonate substitution between the ND and HFD at 16 weeks of age. However, ND had a higher mineral to matrix ratio and carbonate substitution compared to FHFD at 24 weeks of age ($p = 0.0025$). (Figure 8)

There was no significant difference in fluorescent AGES among groups (Figure 9).

Discussion

Adolescent obesity has become a global epidemic with lasting impacts on life-long health. Our results demonstrated that obesity induced by HFD reduced the bone volume fraction of trabecular bone in adolescent mice, which is in agreement with other murine diet-induced obesity studies [21]–[24]. Interestingly if diet induced obesity begins after 11 to 12 weeks age, trabecular volume fraction is higher in obese mice than healthy weight mice [12], [25], indicating obesity during skeletal development has different effects on bone than obesity in mature bone. The trabecular structural degradation remained through skeletal maturity even after the mice returned to normal weight as was found in previous studies [12]. Though trabecular bone volume fraction was reduced, cortical bone was more robust in obese adolescent mice (increased second moment of area and diameter) in agreement with previous studies [10], [11], [13]. Interestingly one previous study found no change in cortical parameters at midshaft in HFD mice [26], but only measured cortical area, not moment of area, which is likely more indicative of periosteal bone formation in obese mice. The increase in cortical size was also maintained through skeletal maturity and return to normal weight. With limited capacity to build bone, the reduction in trabecular bone may be a compensatory effect of increased cortical bone and warrants further investigation of the cortical/trabecular trade off during skeletal development. Nonetheless, it is striking (and concerning) that skeletal structure during adolescents had a lasting impact into adulthood even after the weight is “corrected”.

Our results indicated that the elastic behavior of bone was not altered by adolescent obesity similar to previous studies [23], but the post-yield behavior was reduced with adolescent HFD mice having more brittle behavior than ND mice. Interestingly as the mice aged (and the HFD obtained normal weight), the post-yield behavior was the same between the FHFD and ND groups. Bone naturally becomes more brittle with age [27] and the ND group increased in brittleness (decreased in plastic energy to fracture) between 16 and 24 weeks of age.

In normal, healthy bone, the increase in brittleness with age is caused in part by an increase in mineral/matrix ratio and an increase in non-enzymatic crosslinking (advanced glycation end products, AGEs) [27], [28]. The adolescent (16 week) bones in our study showed no difference in composition between HFD and ND by Raman spectroscopy and AGE analysis. Older (24 week) FHFD bones demonstrated lower mineral to matrix ratio and carbonate substitution compared to ND but had no difference in fluorescent AGEs. Ionova-Martin *et al.* found increased AGEs in adult HFD mice compared to ND mice but not in young HFD mice [13]. Our data indicate when young mice are fed HFD and then switched to ND, fluorescent AGEs are equivalent to ND mice. It is intriguing that the change in mechanics in the 16 week bones was not accompanied by a change in composition (at least in the measures we performed), but in the 24 week old bones when mechanics were similar, composition between the two groups was not. The mechanical integrity of bone is a function of structure, composition, and a myriad of other factors. Changes in mechanical properties are not always directly related to compositional measures. This study indicates that obesity changes the mechanics of bone as well as its composition.

Is obesity accelerating the aging process? Decreased trabecular bone, increased cortical diameter, and reduced ductility (increased brittleness) are characteristics of aging bone and obese bone. It has been suggested that obesity accelerates aging in other organs such as the vessels [29] and brain [30] and may be driven by oxidative stress [31]. Future work will examine other factors of obese adolescent bones which may indicate accelerated aging, such as increased cellular senescence.

In this study we used three-point bending flexural test to estimate material properties (elastic modulus, yield and ultimate stress), requiring the assumptions of small deformation, homogeneous, isotropic, continuous, linear elastic material, straight section after deformation and constant cross section area, none of which are met by the femur. However, when bones are of significantly different moment of area, it is insufficient to compare force-displacement curves, which conflate the influence of geometry and material properties, and assuming Bernoulli bending provides an estimate of material properties. Our compositional measures obtained with Raman spectroscopy and fluorescence assay for AGEs only measure selective portions of bone composition and may not have captured all compositional changes. In addition the 60 kcal % fat diet, though a common animal model of obesity, may not be representative of human obesity.

In conclusion, changes to bone structure and composition were found in mice that recovered from obesity. Childhood is a period of significant skeletal development, the importance of treating childhood obesity to induce a loss of weight is well known [32], [33]. This research has demonstrated that adolescent murine obesity alters structural, mechanical and compositional properties of the bone, which may have lasting implication on bone health even after the obesity is corrected. This finding has broad implications addressing the childhood obesity epidemic.

Acknowledgements

We would like to acknowledge Man I Wu and Michael Albro from Boston University for their assistance in Raman spectroscopy measurements. This work was supported by an Honors Research Fellowship from Northeastern University.

References

[1] C. M. Hales, M. D. Carroll, C. D. Fryar, and C. L. Ogden, "Prevalence of Obesity Among Adults and Youth: United States, 2015-2016.," *NCHS Data Brief*, no. 288, pp. 1–8, Oct. 2017.

[2] D. A. Bailey, H. A. McKay, R. L. Mirwald, P. R. Crocker, and R. A. Faulkner, "A six-year longitudinal study of the relationship of physical activity to bone mineral accrual in growing children: the university of Saskatchewan bone mineral accrual study.," *J. bone Miner. Res. Off. J. Am. Soc. Bone Miner. Res.*, vol. 14, no. 10, pp. 1672–1679, Oct. 1999, doi: 10.1359/jbmr.1999.14.10.1672.

[3] P. Dimitri, N. Bishop, J. S. Walsh, and R. Eastell, "Obesity is a risk factor for fracture in children but is protective against fracture in adults: a paradox.," *Bone*, vol. 50, no. 2, pp. 457–466, Feb. 2012, doi: 10.1016/j.bone.2011.05.011.

[4] C. De Laet *et al.*, "Body mass index as a predictor of fracture risk: a meta-analysis.," *Osteoporos. Int. a J. Establ. as result Coop. between Eur. Found. Osteoporos. Natl. Osteoporos. Found. USA*, vol. 16, no. 11, pp. 1330–1338, Nov. 2005, doi: 10.1007/s00198-005-1863-y.

[5] A. Ivuskans *et al.*, "Bone mineral density in 11-13-year-old boys: relative importance of the weight status and body composition factors.," *Rheumatol. Int.*, vol. 33, no. 7, pp. 1681–1687, Jul. 2013, doi: 10.1007/s00296-012-2612-0.

[6] K. J. Ellis, R. J. Shypailo, W. W. Wong, and S. A. Abrams, "Bone mineral mass in overweight and obese children: diminished or enhanced?," *Acta Diabetol.*, vol. 40 Suppl 1, pp. S274-7, Oct. 2003, doi: 10.1007/s00592-003-0085-z.

[7] M. B. Leonard, J. Shults, B. A. Wilson, A. M. Tershakovec, and B. S. Zemel, "Obesity during childhood and adolescence augments bone mass and bone dimensions.," *Am. J. Clin. Nutr.*, vol. 80, no. 2, pp. 514–523, Aug. 2004, doi: 10.1093/ajcn/80.2.514.

[8] D. C. Perry, D. Metcalfe, M. L. Costa, and T. Van Staa, "A nationwide cohort study of slipped capital femoral epiphysis.," *Arch. Dis. Child.*, vol. 102, no. 12, pp. 1132–1136, Dec. 2017, doi: 10.1136/archdischild-2016-312328.

[9] V. Brahmabhatt, J. Rho, L. Bernardis, R. Gillespie, and I. Ziv, "The effects of dietary-induced obesity on the biomechanical properties of femora in male rats," *Int. J. Obes. Relat. Metab. Disord.*, vol. 22, no. 8, p. 813—818, 1998, doi: 10.1038/sj.ijo.0800668.

[10] M. J. Devlin *et al.*, "Differential effects of high fat diet and diet-induced obesity on skeletal acquisition in female C57BL/6J vs. FVB/NJ Mice.," *Bone reports*, vol. 8, pp. 204–214, Jun. 2018, doi: 10.1016/j.bonr.2018.04.003.

[11] S. S. Ionova-Martin *et al.*, "Reduced size-independent mechanical properties of cortical bone in high-fat diet-induced obesity.," *Bone*, vol. 46, no. 1, pp. 217–225, Jan. 2010, doi: 10.1016/j.bone.2009.10.015.

[12] J. A. Inzana *et al.*, "Immature mice are more susceptible to the detrimental effects of high fat diet on cancellous bone in the distal femur.," *Bone*, vol. 57, no. 1, pp. 174–183, Nov. 2013, doi: 10.1016/j.bone.2013.08.003.

[13] S. S. Ionova-Martin *et al.*, "Changes in cortical bone response to high-fat diet from adolescence to adulthood in mice.," *Osteoporos. Int. a J. Establ. as result Coop. between Eur. Found. Osteoporos. Natl. Osteoporos. Found. USA*, vol. 22, no. 8, pp. 2283–2293, Aug. 2011, doi: 10.1007/s00198-010-1432-x.

[14] P. Dimitri, "The Impact of Childhood Obesity on Skeletal Health and Development," *J. Obes. Metab. Syndr.*, vol. 28, no. 1, pp. 4–17, Mar. 2019, doi: 10.7570/jomes.2019.28.1.4.

[15] V. Glatt, E. Canalis, L. Stadmeyer, and M. L. Bouxsein, "Age-related changes in trabecular architecture differ in female and male C57BL/6J mice.," *J. bone Miner. Res. Off. J. Am. Soc.*

Bone Miner. Res., vol. 22, no. 8, pp. 1197–1207, Aug. 2007, doi: 10.1359/jbmr.070507.

[16] C. A. Schneider, W. S. Rasband, and K. W. Eliceiri, "NIH Image to ImageJ: 25 years of image analysis.," *Nat. Methods*, vol. 9, no. 7, pp. 671–675, Jul. 2012, doi: 10.1038/nmeth.2089.

[17] M. Doube *et al.*, "BoneJ: Free and extensible bone image analysis in ImageJ.," *Bone*, vol. 47, no. 6, pp. 1076–1079, Dec. 2010, doi: 10.1016/j.bone.2010.08.023.

[18] Bruker-microCT, *Morphometric parameters measured by Skyscan ™ CT - analyser software* . 2012.

[19] M. Jensen, C. C. Horgan, T. Vercauteren, M. B. Albro, and M. S. Bergholt, "Multiplexed polarized hypodermic Raman needle probe for biostructural analysis of articular cartilage," *Opt. Lett.*, vol. 45, no. 10, pp. 2890–2893, 2020, doi: 10.1364/OL.390998.

[20] S. Mehta, S. Akhtar, R. M. Porter, P. Önnerfjord, and A. G. Bajpayee, "Interleukin-1 receptor antagonist (IL-1Ra) is more effective in suppressing cytokine-induced catabolism in cartilage-synovium co-culture than in cartilage monoculture.," *Arthritis Res. Ther.*, vol. 21, no. 1, p. 238, Nov. 2019, doi: 10.1186/s13075-019-2003-y.

[21] S. Mehta *et al.*, "Resveratrol and Curcumin Attenuate Ex Vivo Sugar-Induced Cartilage Glycation, Stiffening, Senescence, and Degeneration," *Cartilage*, p. 1947603520988768, Jan. 2021, doi: 10.1177/1947603520988768.

[22] J. F. Woessner, "The determination of hydroxyproline in tissue and protein samples containing small proportions of this imino acid," *Arch. Biochem. Biophys.*, vol. 93, no. 2, pp. 440–447, 1961, doi: https://doi.org/10.1016/0003-9861(61)90291-0.

[23] M. J. Devlin *et al.*, "Early-Onset Type 2 Diabetes Impairs Skeletal Acquisition in the Male TALLYHO/JngJ Mouse," *Endocrinology*, vol. 155, no. 10, pp. 3806–3816, Oct. 2014, doi: 10.1210/en.2014-1041.

[24] J. J. Cao, L. Sun, and H. Gao, "Diet-induced obesity alters bone remodeling leading to decreased femoral trabecular bone mass in mice.," *Ann. N. Y. Acad. Sci.*, vol. 1192, pp. 292–297, Mar. 2010, doi: 10.1111/j.1749-6632.2009.05252.x.

[25] M. Tencerova, F. Figeac, N. Ditzel, H. Taipaleenmäki, T. K. Nielsen, and M. Kassem, "High-Fat Diet-Induced Obesity Promotes Expansion of Bone Marrow Adipose Tissue and Impairs Skeletal Stem Cell Functions in Mice.," *J. bone Miner. Res. Off. J. Am. Soc. Bone Miner. Res.*, vol. 33, no. 6, pp. 1154–1165, Jun. 2018, doi: 10.1002/jbmr.3408.

[26] C. R. Doucette *et al.*, "A High Fat Diet Increases Bone Marrow Adipose Tissue (MAT) But Does Not Alter Trabecular or Cortical Bone Mass in C57BL/6J Mice.," *J. Cell. Physiol.*, vol. 230, no. 9, pp. 2032–2037, Sep. 2015, doi: 10.1002/jcp.24954.

[27] R. K. Nalla, J. J. Kruzic, J. H. Kinney, and R. O. Ritchie, "Effect of aging on the toughness of human cortical bone: evaluation by R-curves.," *Bone*, vol. 35, no. 6, pp. 1240–1246, Dec. 2004, doi: 10.1016/j.bone.2004.07.016.

[28] E. Fornari, M. Suszter, J. Roocroft, T. Bastrom, E. Edmonds, and J. Schlechter, "Childhood Obesity as a Risk Factor for Lateral Condyle Fractures Over Supracondylar Humerus Fractures," *Clin. Orthop. Relat. Res.*, vol. 471, Sep. 2012, doi: 10.1007/s11999-012-2566-2.

[29] M. Barton, O. Baretella, and M. R. Meyer, "Obesity and risk of vascular disease: importance of endothelium-dependent vasoconstriction.," *Br. J. Pharmacol.*, vol. 165, no. 3, pp. 591–602, Feb. 2012, doi: 10.1111/j.1476-5381.2011.01472.x.

[30] Z. Tucsek *et al.*, "Obesity in aging exacerbates blood-brain barrier disruption, neuroinflammation, and oxidative stress in the mouse hippocampus: effects on expression of genes involved in beta-amyloid generation and Alzheimer's disease.," *J. Gerontol. A. Biol. Sci. Med. Sci.*, vol. 69, no. 10, pp. 1212–1226, Oct. 2014, doi: 10.1093/gerona/glt177.

[31] A. B. Salmon, "Beyond Diabetes: Does Obesity-Induced Oxidative Stress Drive the Aging Process?," *Antioxidants (Basel, Switzerland)*, vol. 5, no. 3, Jul. 2016, doi: 10.3390/antiox5030024.

[32] M. Ho *et al.*, "Effectiveness of lifestyle interventions in child obesity: systematic review with meta-analysis.," *Pediatrics*, vol. 130, no. 6, pp. e1647-71, Dec. 2012, doi: 10.1542/peds.2012-1176.

[33] L. H. Epstein, R. A. Paluch, J. N. Roemmich, and M. D. Beecher, "Family-based obesity treatment, then and now: twenty-five years of pediatric obesity treatment.," *Heal. Psychol. Off. J. Div. Heal. Psychol. Am. Psychol. Assoc.*, vol. 26, no. 4, pp. 381–391, Jul. 2007, doi: 10.1037/0278-6133.26.4.381.

[34] Elizabeth Rendina-Ruedy, 1. K. (2015). A comparative study of the metabolic and skeletal response of C57BL/6J and C57BL/6N mice in a diet-induced model of type 2 diabetes. *Journal of Nutrition and Metabolism*.

[35] JJ Cao, B. G. (2009). High-fat diet decreases cancellous bone mass but has no effect on cortical bone mass in the tibia in mice. *Bone*, 1097-1104.

Figure Legends:

Figure 1. 2D Micro-CT images showing regions of trabecular bone evaluation in the femur: (A) region of interest for trabecular bone analysis and (B) region of interest for cortical bone analysis.

Figure 2. Average weights of mice over time (mean ± s.d.). The weights of the ND mice were significantly different from the weights of the HFD mice from 8-16 weeks of age after applying the Bonferroni correction for multiple comparisons (**α**=0.0036) and from 16-24 weeks no significant difference in weight was found.

Figure 3. Weight of gonadal fat pads of mice groups over time. The weights of the ND mice were significantly different from the fat pads of the 16 weeks old mice HFD mice, and not significantly different between the ND 24 weeks and the FHFD. Box plots indicate 25-75%, st. deviation and median.

Figure 4: Micro-CT analysis of trabecular bone in the distal femur. Trabecular bone parameters were evaluated as trabecular thickness (A), trabecular separation (B), trabecular number (C) and trabecular bone volume fraction (D). *$p < 0.05$, HFD or FHFD versus same age ND. Box plots indicate 25-75%, st. deviation and median.

Figure 5: Representative Micro-CT images of the trabecular bone area of distal femur from a 16-week-old normal diet mice (A), a 16-week-old high fat diet mice (B), a 24-week-old normal diet mice (C) and a 24 week-old former high fat diet mice. These images were captured with a 7 μm resolution for illustrative purposes.

Figure 6: For each plot, top box is the variation of a parameter along the bone, presented as mean (line) and standard deviation (shaded area). The box below indicates regions of significant difference between the two groups ($p<0.05$). The parameters studied are: (A) Mean cross sectional area (CSA), (B) Mean I_{ML}, and (C) Mean D_{ML}.

Figure 7: A) Representative stress and strain curve of HFD, FHFD and ND mice at 16 and 24 weeks of age. B) HFD mice have a higher ultimate stress than the 16 weeks old ND (*$p = 0.007$) whereas the

408 FHFD have an equivalent ultimate stress. C) HFD mice and FHFD have equivalent elastic modulus as the
409 group control. D) HFD have a lower ductility than the 16 weeks old ND (*p= 0.004) whereas FHFD are
410 equivalent to the ND at 24 weeks old. Box plots indicate 25-75%, st. deviation and median.

411 **Figure 8:** Raman Spectroscopy results. A) There was no significant difference in mineral to matrix ratio
412 between the ND and HFD. However, ND had a higher mineral content than the FHFD of the same age
413 (*p = 0.0025). B) There was no significant difference in carbonate substitution between the ND and HFD.
414 There was a significantly higher carbonate substitution for the ND than the FHFD of the same age (*p =
415 0.0025). Box plots indicate 25-75%, st. deviation and median.

416 **Figure 9:** There was no significant difference in fluorescent AGE between groups. Box plots indicate
417 25-75%, st. deviation and median.

418

419 **Figures**

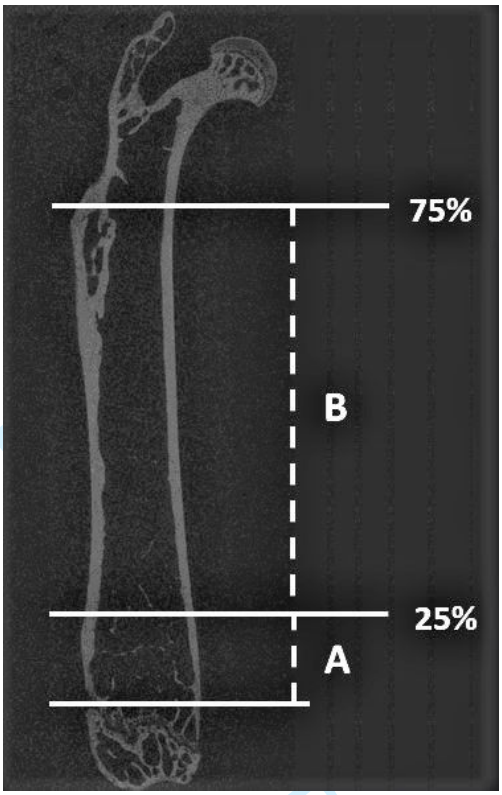

420

421 **Figure 1:** 2D Micro-CT images showing regions of trabecular bone evaluation in the femur: (A) region of

422 interest for trabecular bone analysis and (B) region of interest for cortical bone analysis.

423

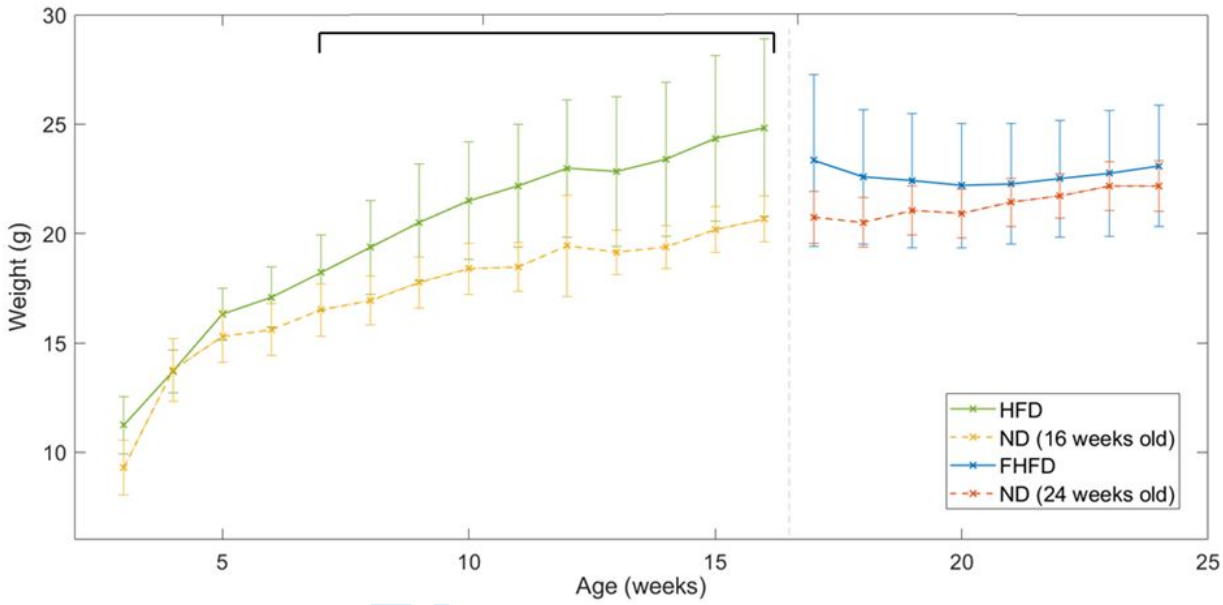

Figure 2. Average weights of mice over time (mean ± s.d.). The weights of the ND mice were significantly different from the weights of the HFD mice from 8-16 weeks of age after applying the Bonferroni correction for multiple comparisons (**α**=0.0036) and from 16-24 weeks no significant difference in weight was found.

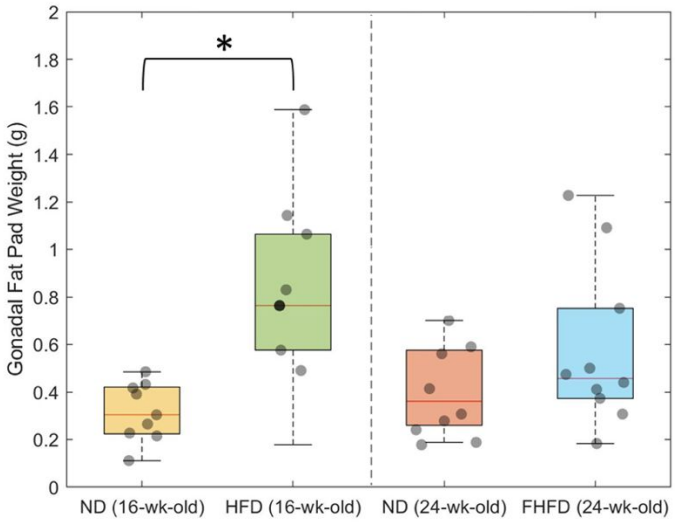

424 **Figure 3.** Weight of gonadal fat pads of mice groups over time. The weights of the ND mice were

425 significantly different from the fat pads of the 16 weeks old mice HFD mice, and not significantly

426 different between the ND 24 weeks and the FHFD. Box plots indicate 25-75%, st. deviation and median.

427

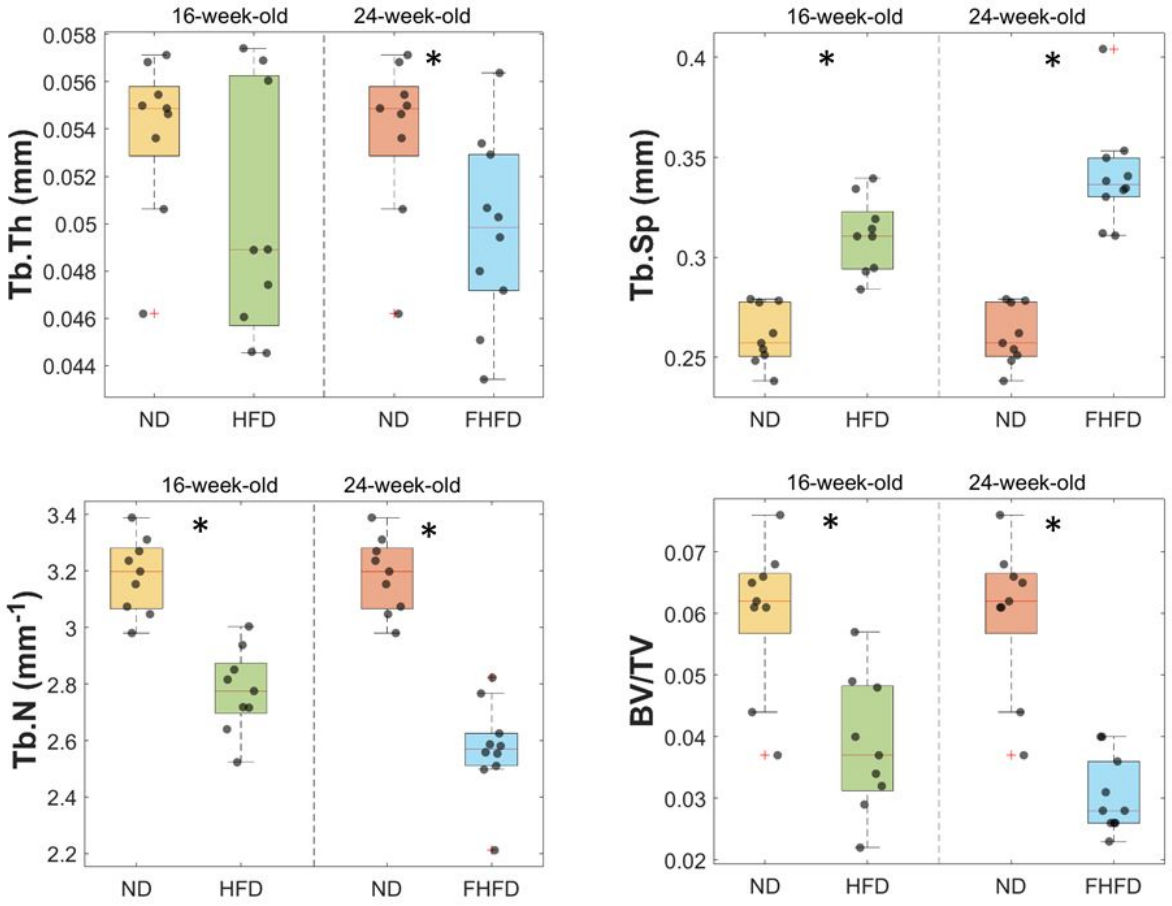

Figure 4: Micro-CT analysis of trabecular bone in the distal femur. Trabecular bone parameters were evaluated as trabecular thickness (A), trabecular separation (B), trabecular number (C) and trabecular bone volume fraction (D). *$p < 0.05$, HFD or FHFD versus same age ND. Box plots indicate 25-75%, st. deviation and median.

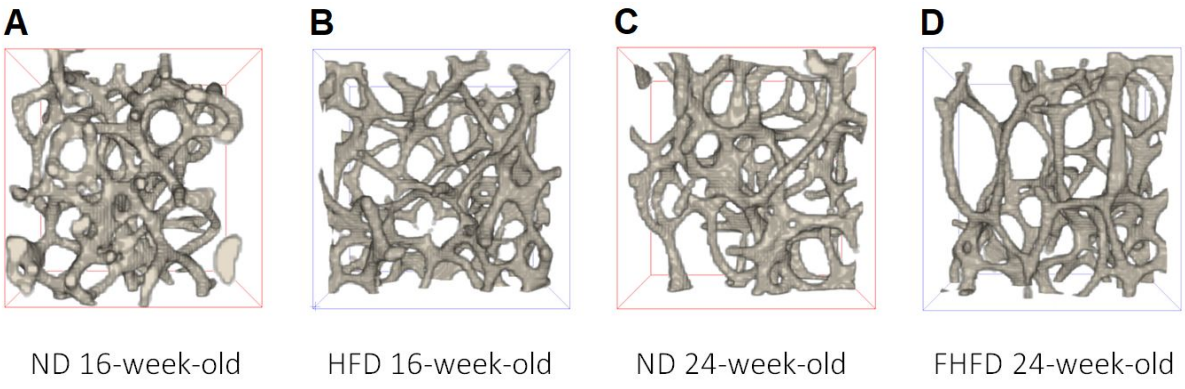

Figure 5: Representative Micro-CT images of the trabecular bone area of distal femur from a 16-week-old normal diet mice (A), a 16-week-old high fat diet mice (B), a 24-week-old normal diet mice (C) and a 24 week-old former high fat diet mice. These images were captured with a 7 µm resolution for illustrative purposes.

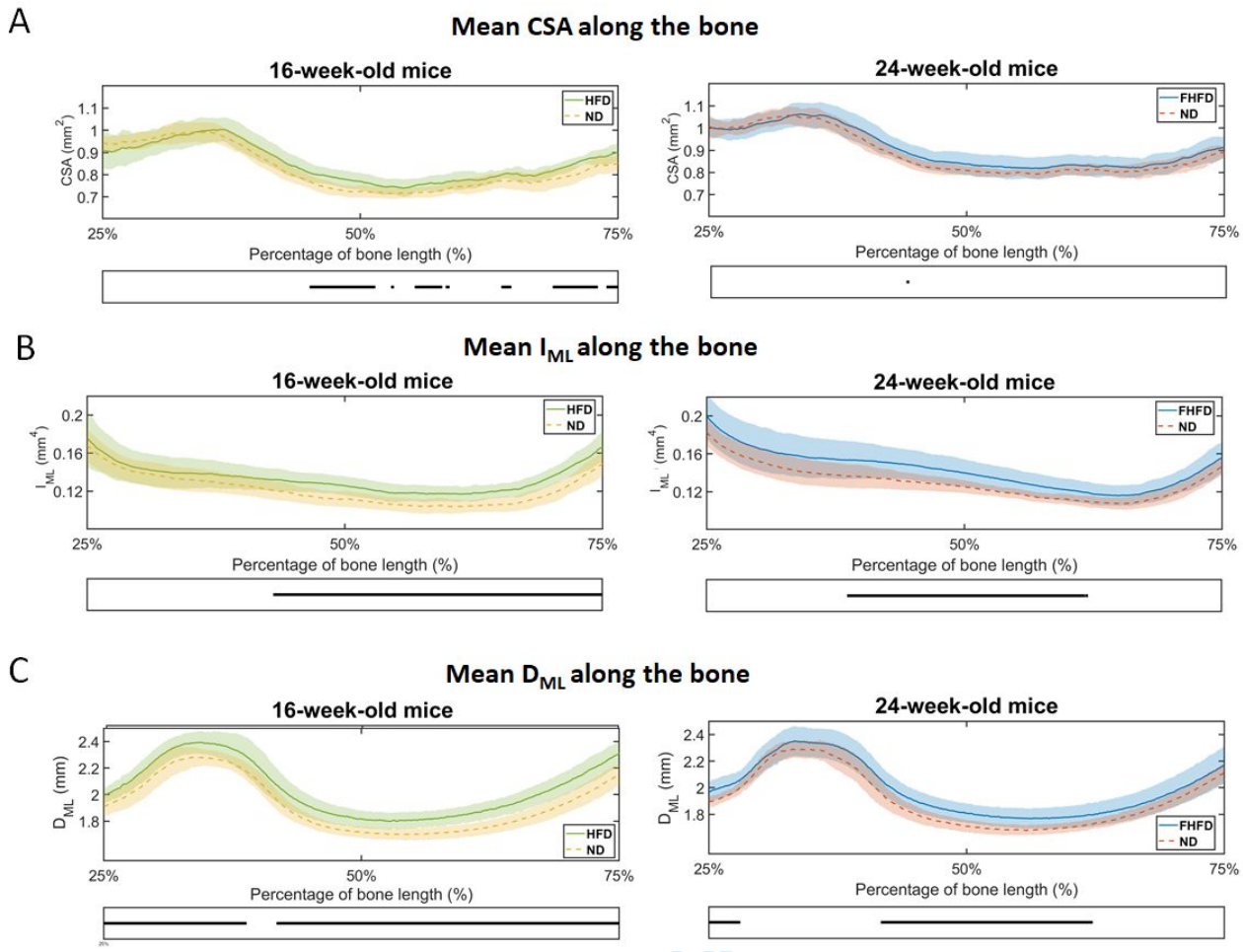

Figure 6: For each plot, top box is the variation of a parameter along the bone, presented as mean (line) and standard deviation (shaded area). The box below indicates regions of significant difference between the two groups ($p<0.05$). The parameters studied are: (A) Mean cross sectional area (CSA), (B) Mean I_{ML}, and (C) Mean D_{ML}.

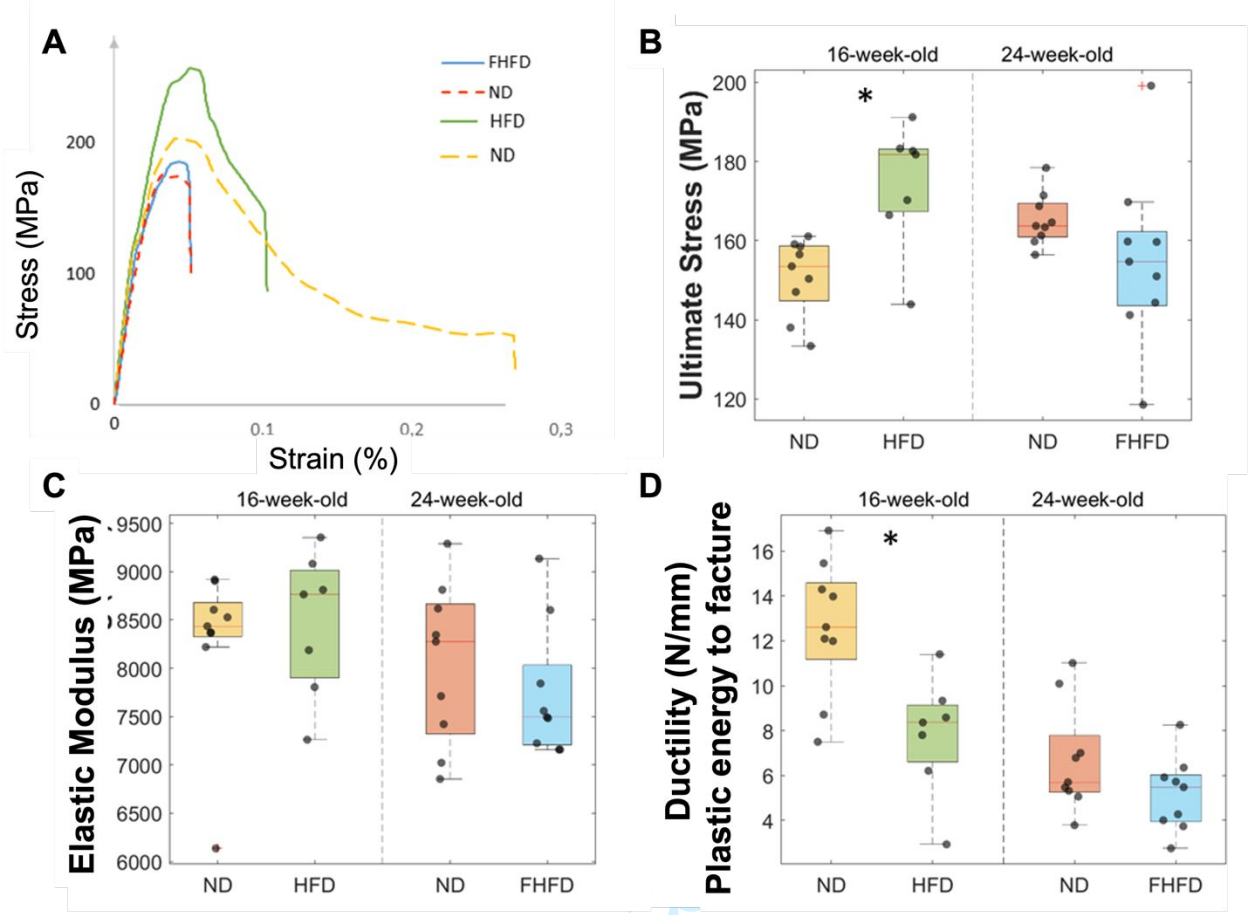

Figure 7: A) Representative stress and strain curve of HFD, FHFD and ND mice at 16 and 24 weeks of age. B) HFD mice have a higher ultimate stress than the 16 weeks old ND (*p = 0.007) whereas the FHFD have an equivalent ultimate stress. C) HFD mice and FHFD have equivalent elastic modulus as the group control. D) HFD have a lower ductility than the 16 weeks old ND (*p= 0.004) whereas FHFD are equivalent to the ND at 24 weeks old. Box plots indicate 25-75%, st. deviation and median.

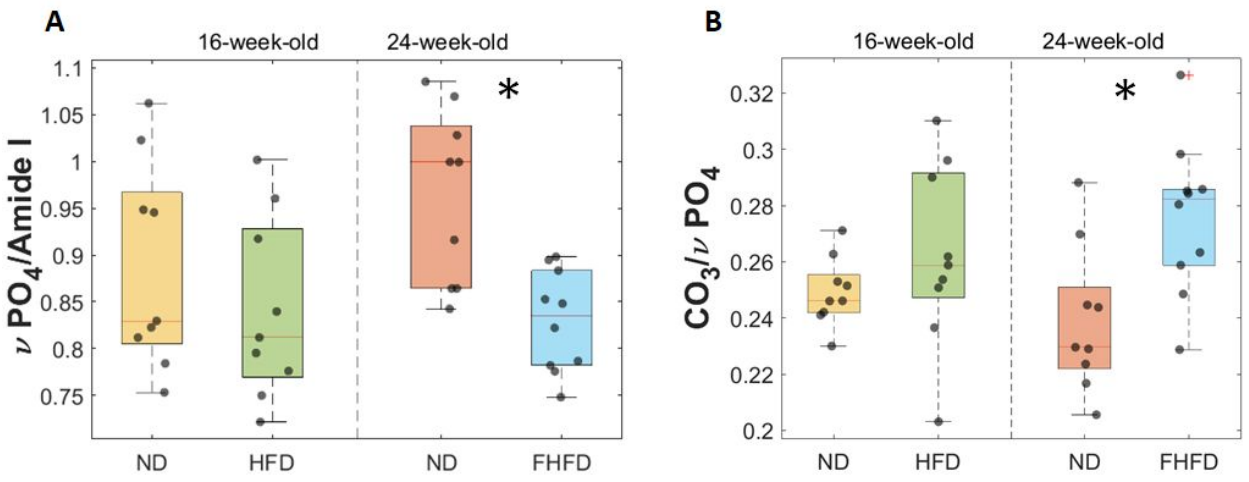

Figure 8: Raman Spectroscopy results. A) There was no significant difference in mineral to matrix ratio between the ND and HFD. However, ND had a higher mineral content than the FHFD of the same age (*p = 0.0025). B) There was no significant difference in carbonate substitution between the ND and HFD. There was a significantly higher carbonate substitution for the ND than the FHFD of the same age (*p = 0.0025). Box plots indicate 25-75%, st. deviation and median.

462

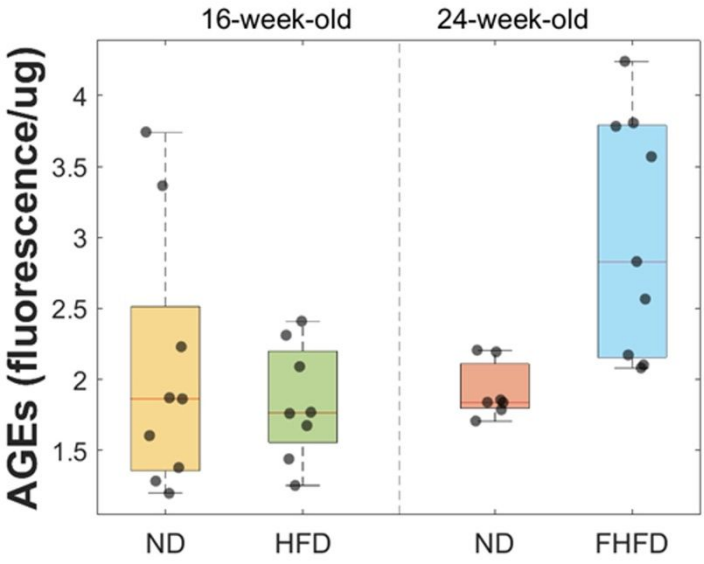

463

464 **Figure 9:** There was no significant difference in fluorescent AGE between groups. Box plots indicate 25-

465 75%, st. deviation and median.

466

467

ARRIVE

The ARRIVE Guidelines Checklist

Animal Research: Reporting In Vivo Experiments

Carol Kilkenny[1], William J Browne[2], Innes C Cuthill[3], Michael Emerson[4] and Douglas G Altman[5]

[1]The National Centre for the Replacement, Refinement and Reduction of Animals in Research, London, UK, [2]School of Veterinary Science, University of Bristol, Bristol, UK, [3]School of Biological Sciences, University of Bristol, Bristol, UK, [4]National Heart and Lung Institute, Imperial College London, UK, [5]Centre for Statistics in Medicine, University of Oxford, Oxford, UK.

	ITEM	RECOMMENDATION	Section/ Paragraph
Title	1	Provide as accurate and concise a description of the content of the article as possible.	title page
Abstract	2	Provide an accurate summary of the background, research objectives, including details of the species or strain of animal used, key methods, principal findings and conclusions of the study.	p. 2
INTRODUCTION			
Background	3	a. Include sufficient scientific background (including relevant references to previous work) to understand the motivation and context for the study, and explain the experimental approach and rationale. b. Explain how and why the animal species and model being used can address the scientific objectives and, where appropriate, the study's relevance to human biology.	line 56-65
Objectives	4	Clearly describe the primary and any secondary objectives of the study, or specific hypotheses being tested.	line 66
METHODS			
Ethical statement	5	Indicate the nature of the ethical review permissions, relevant licences (e.g. Animal [Scientific Procedures] Act 1986), and national or institutional guidelines for the care and use of animals, that cover the research.	line 74
Study design	6	For each experiment, give brief details of the study design including: a. The number of experimental and control groups. b. Any steps taken to minimise the effects of subjective bias when allocating animals to treatment (e.g. randomisation procedure) and when assessing results (e.g. if done, describe who was blinded and when). c. The experimental unit (e.g. a single animal, group or cage of animals). A time-line diagram or flow chart can be useful to illustrate how complex study designs were carried out.	line 72-78
Experimental procedures	7	For each experiment and each experimental group, including controls, provide precise details of all procedures carried out. For example: a. How (e.g. drug formulation and dose, site and route of administration, anaesthesia and analgesia used [including monitoring], surgical procedure, method of euthanasia). Provide details of any specialist equipment used, including supplier(s). b. When (e.g. time of day). c. Where (e.g. home cage, laboratory, water maze). d. Why (e.g. rationale for choice of specific anaesthetic, route of administration, drug dose used).	line 72-78
Experimental animals	8	a. Provide details of the animals used, including species, strain, sex, developmental stage (e.g. mean or median age plus age range) and weight (e.g. mean or median weight plus weight range). b. Provide further relevant information such as the source of animals, international strain nomenclature, genetic modification status (e.g. knock-out or transgenic), genotype, health/immune status, drug or test naïve, previous procedures, etc.	line 72-78

The ARRIVE guidelines. Originally published in *PLoS Biology*, June 2010[1]

Housing and husbandry	9	Provide details of: a. Housing (type of facility e.g. specific pathogen free [SPF]; type of cage or housing; bedding material; number of cage companions; tank shape and material etc. for fish). b. Husbandry conditions (e.g. breeding programme, light/dark cycle, temperature, quality of water etc for fish, type of food, access to food and water, environmental enrichment). c. Welfare-related assessments and interventions that were carried out prior to, during, or after the experiment.	line 72-78
Sample size	10	a. Specify the total number of animals used in each experiment, and the number of animals in each experimental group. b. Explain how the number of animals was arrived at. Provide details of any sample size calculation used. c. Indicate the number of independent replications of each experiment, if relevant.	line 72-78
Allocating animals to experimental groups	11	a. Give full details of how animals were allocated to experimental groups, including randomisation or matching if done. b. Describe the order in which the animals in the different experimental groups were treated and assessed.	line 72-78
Experimental outcomes	12	Clearly define the primary and secondary experimental outcomes assessed (e.g. cell death, molecular markers, behavioural changes).	line 84-154
Statistical methods	13	a. Provide details of the statistical methods used for each analysis. b. Specify the unit of analysis for each dataset (e.g. single animal, group of animals, single neuron). c. Describe any methods used to assess whether the data met the assumptions of the statistical approach.	line 156-178
RESULTS			
Baseline data	14	For each experimental group, report relevant characteristics and health status of animals (e.g. weight, microbiological status, and drug or test naïve) prior to treatment or testing. (This information can often be tabulated).	line 184-186, figure 2
Numbers analysed	15	a. Report the number of animals in each group included in each analysis. Report absolute numbers (e.g. 10/20, not 50%[2]). b. If any animals or data were not included in the analysis, explain why.	line 72-78
Outcomes and estimation	16	Report the results for each analysis carried out, with a measure of precision (e.g. standard error or confidence interval).	box plots, SD, confidence interval
Adverse events	17	a. Give details of all important adverse events in each experimental group. b. Describe any modifications to the experimental protocols made to reduce adverse events.	none
DISCUSSION			
Interpretation/ scientific implications	18	a. Interpret the results, taking into account the study objectives and hypotheses, current theory and other relevant studies in the literature. b. Comment on the study limitations including any potential sources of bias, any limitations of the animal model, and the imprecision associated with the results[2]. c. Describe any implications of your experimental methods or findings for the replacement, refinement or reduction (the 3Rs) of the use of animals in research.	line 249-269, line 275
Generalisability/ translation	19	Comment on whether, and how, the findings of this study are likely to translate to other species or systems, including any relevance to human biology.	line 285
Funding	20	List all funding sources (including grant number) and the role of the funder(s) in the study.	line 293

References:
1. Kilkenny C, Browne WJ, Cuthill IC, Emerson M, Altman DG (2010) Improving Bioscience Research Reporting: The ARRIVE Guidelines for Reporting Animal Research. *PLoS Biol* 8(6): e1000412. doi:10.1371/journal.pbio.1000412
2. Schulz KF, Altman DG, Moher D, the CONSORT Group (2010) CONSORT 2010 Statement: updated guidelines for reporting parallel group randomised trials. *BMJ* 340:c332.

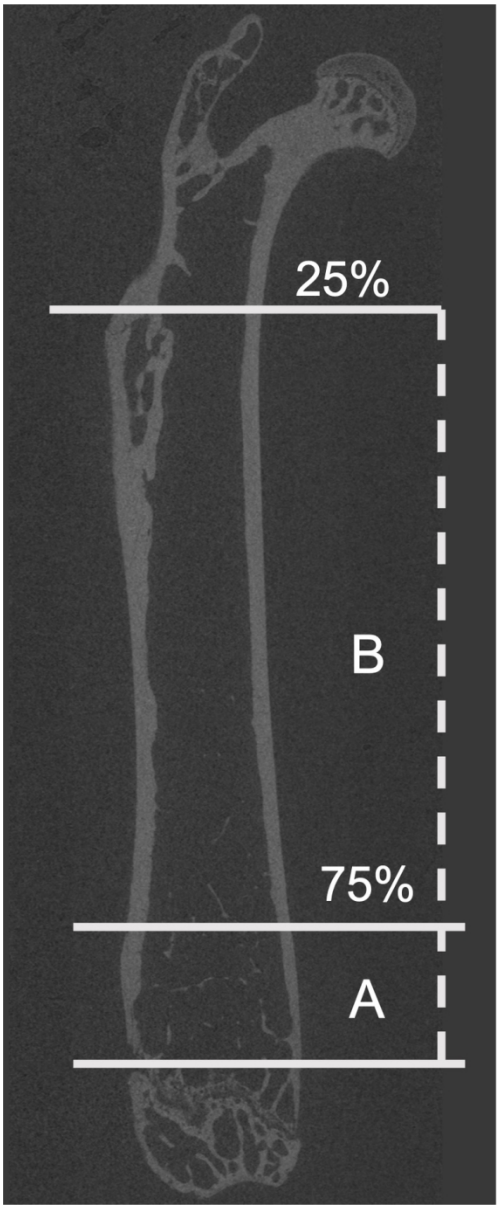

Figure 1: 2D Micro-CT images showing regions of trabecular bone evaluation in the femur: (A) region of interest for trabecular bone analysis and (B) region of interest for cortical bone analysis.

65x158mm (300 x 300 DPI)

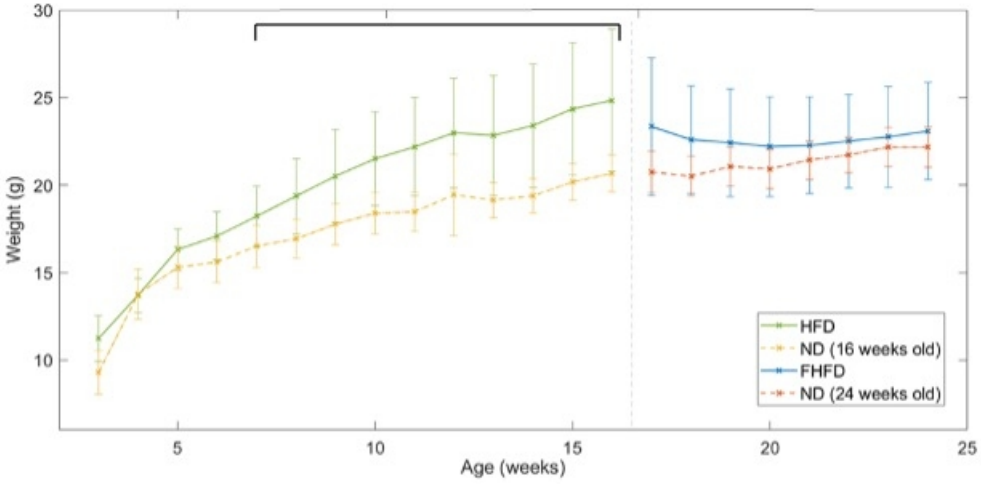

Figure 2. Average weights of mice over time (mean + s.d.). The weights of the ND mice were significantly different from the weights of the HFD mice from 8-16 weeks of age after applying the Bonferroni correction for multiple comparisons (►►=0.0036) and from 16-24 weeks no significant difference in weight was found.

165x81mm (96 x 96 DPI)

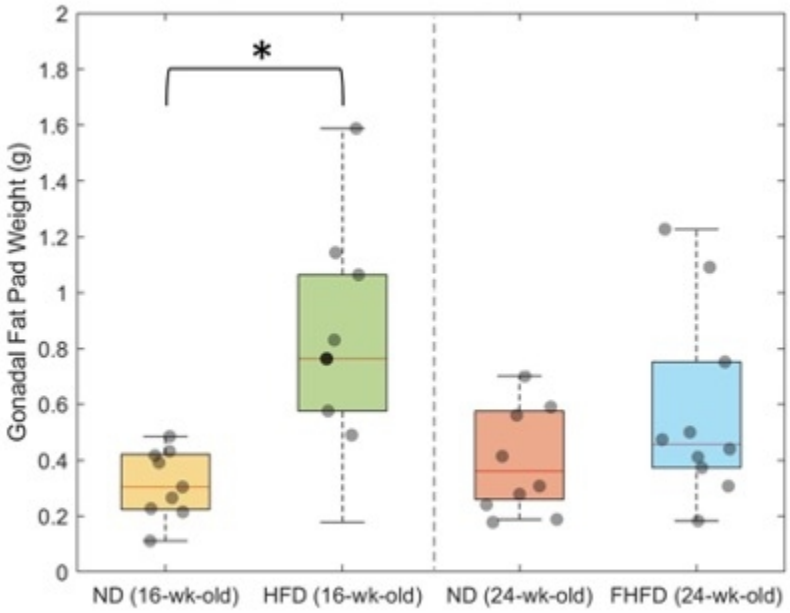

Weight of gonadal fat pads of mice groups over time. The weights of the ND mice were significantly different from the fat pads of the 16 weeks old mice HFD mice, and not significantly different between the ND 24 weeks and the FHFD. Box plots indicate 25-75%, st. deviation and median.

165x123mm (72 x 72 DPI)

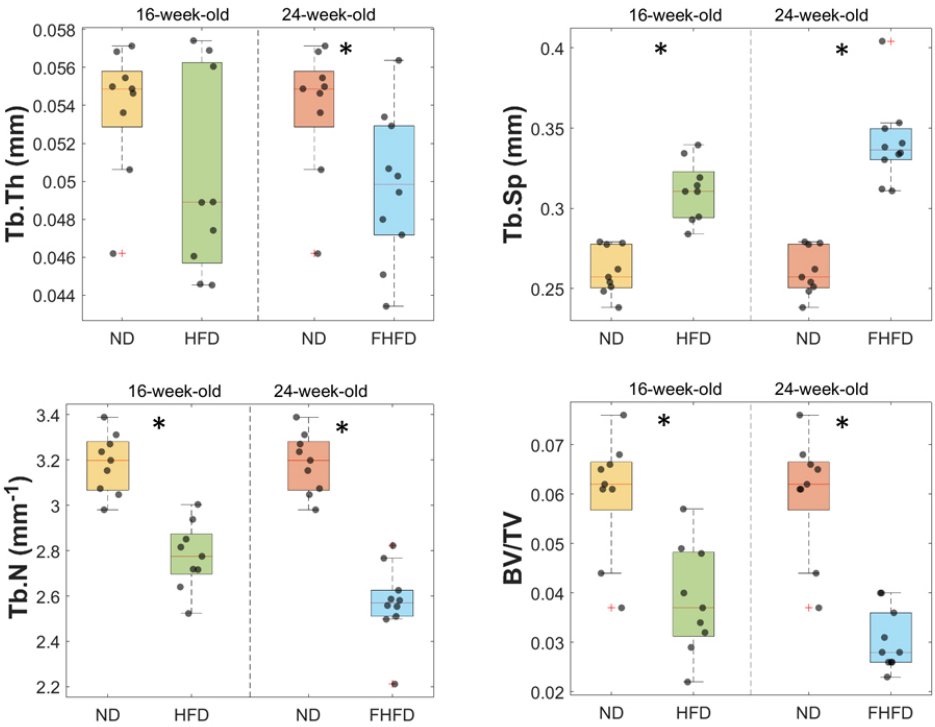

Micro-CT analysis of trabecular bone in the distal femur. Trabecular bone parameters were evaluated as trabecular thickness (A), trabecular separation (B), trabecular number (C) and trabecular bone volume fraction (D). *p < 0.05, HFD or FHFD versus same age ND. Box plots indicate 25-75%, st. deviation and median.

254x190mm (96 x 96 DPI)

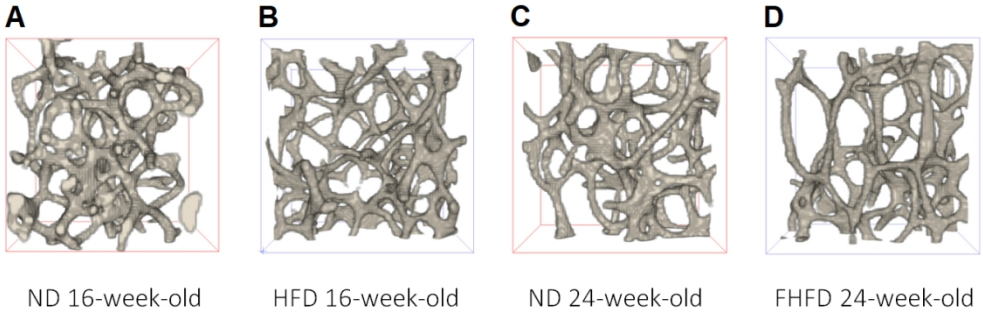

Representative Micro-CT images of the trabecular bone area of distal femur from a 16-week-old normal diet mice (A), a 16-week-old high fat diet mice (B), a 24-week-old normal diet mice (C) and a 24 week-old former high fat diet mice. These images were captured with a 7 μm resolution for illustrative purposes.

288x90mm (120 x 120 DPI)

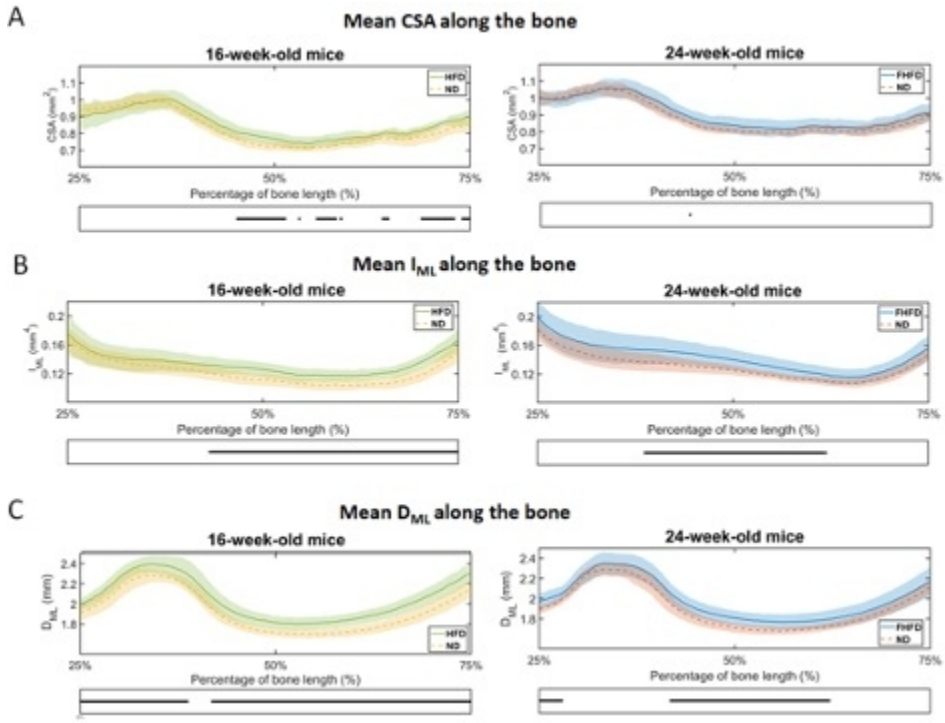

For each plot, top box is the variation of a parameter along the bone, presented as mean (line) and standard deviation (shaded area). The box below indicates regions of significant difference between the two groups ($p<0.05$). The parameters studied are: (A) Mean cross sectional area (CSA), (B) Mean IML, and (C) Mean DML.

165x127mm (72 x 72 DPI)

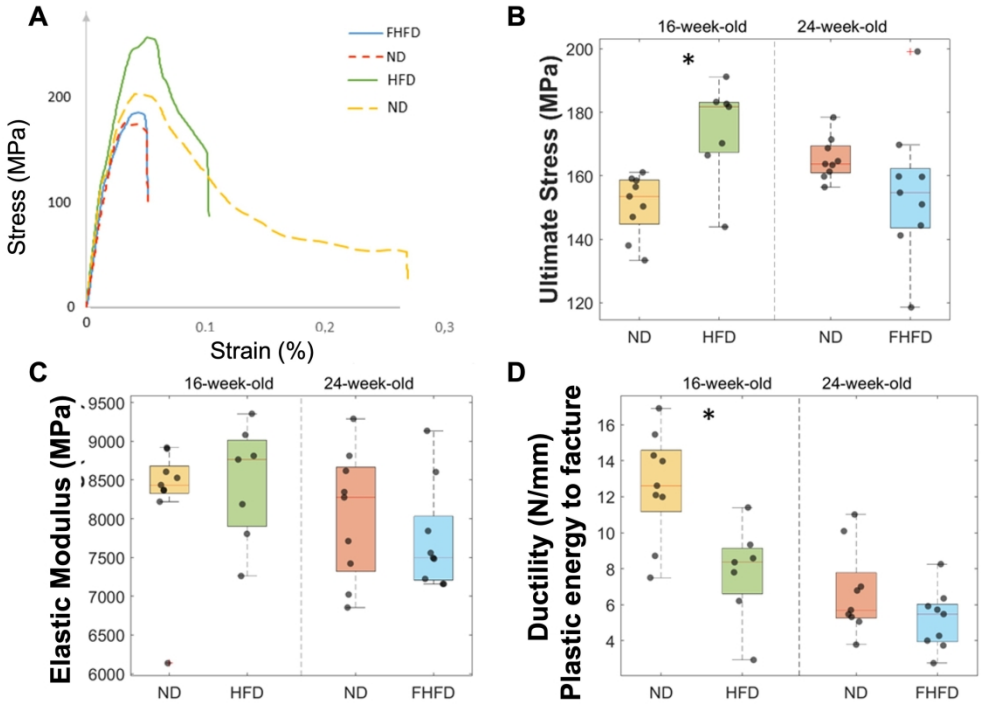

A) Representative stress and strain curve of HFD, FHFD and ND mice at 16 and 24 weeks of age. B) HFD mice have a higher ultimate stress than the 16 weeks old ND (*p = 0.007) whereas the FHFD have an equivalent ultimate stress. C) HFD mice and FHFD have equivalent elastic modulus as the group control. D) HFD have a lower ductility than the 16 weeks old ND (*p= 0.004) whereas FHFD are equivalent to the ND at 24 weeks old. Box plots indicate 25-75%, st. deviation and median.

271x199mm (300 x 300 DPI)

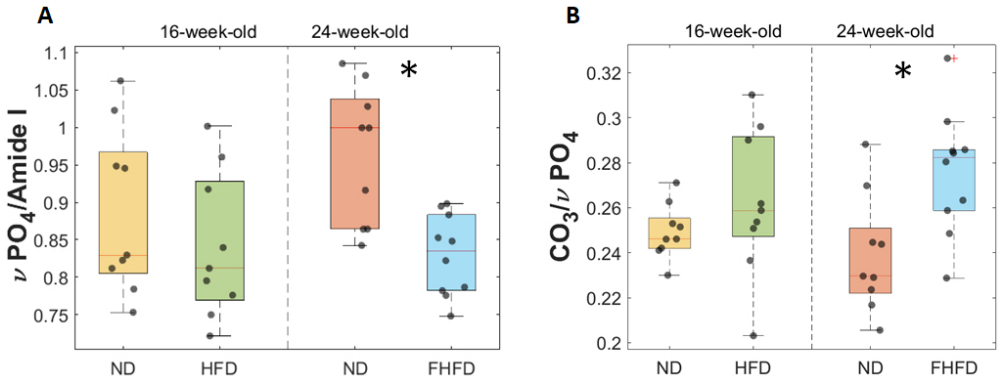

Raman Spectroscopy results. A) There was no significant difference in mineral to matrix ratio between the ND and HFD. However, ND had a higher mineral content than the FHFD of the same age (*p = 0.0025). B) There was no significant difference in carbonate substitution between the ND and HFD. There was a significantly higher carbonate substitution for the ND than the FHFD of the same age (*p = 0.0025). Box plots indicate 25-75%, st. deviation and median.

180x70mm (144 x 144 DPI)

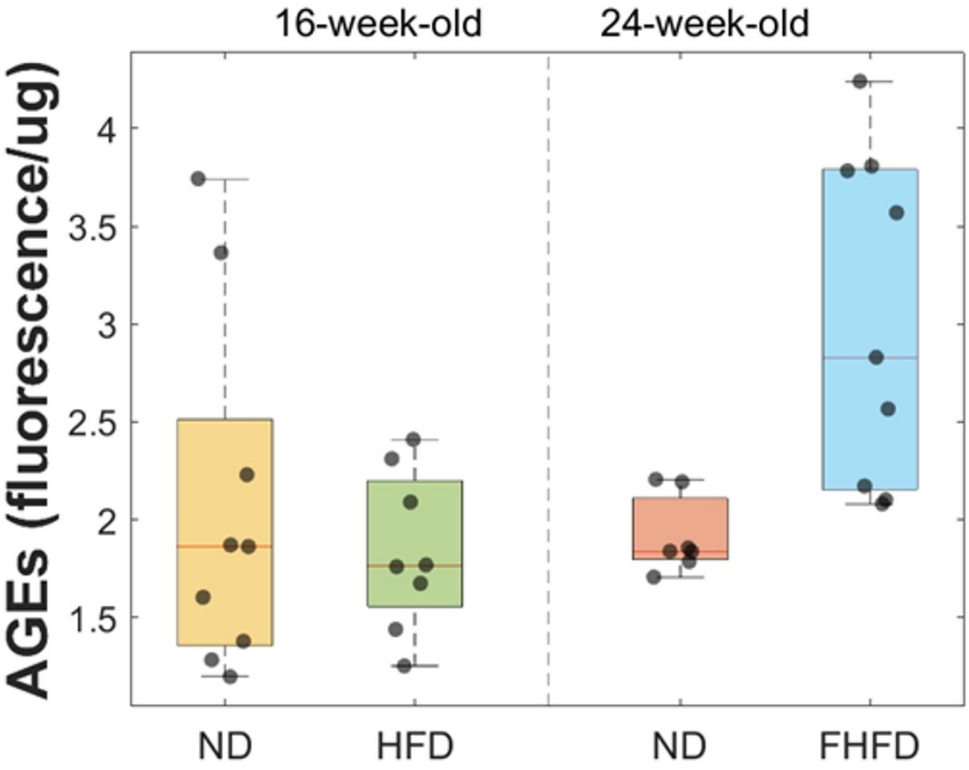

There was no significant difference in fluorescent AGE between groups. Box plots indicate 25-75%, st. deviation and median.

95x76mm (300 x 300 DPI)